Chaos ARTICLE scitation.org/journal/cha

Two-dimensional optical chimera states in an array of coupled waveguide resonators

Cite as: Chaos **30**, 043107 (2020); doi: 10.1063/1.5133836
Submitted: 27 October 2019 · Accepted: 16 March 2020 ·
Published Online: 3 April 2020

View Online Export Citation CrossMark

M. G. Clerc,[1] S. Coulibaly,[2] M. A. Ferré,[1,a)] and M. Tlidi[3]

AFFILIATIONS

[1]Departamento de Física and Millennium Institute for Research in Optics, Facultad de Ciencias Físicas y Matemáticas, Universidad de Chile, Casilla 487-3, Santiago, Chile
[2]Université de Lille, CNRS, UMR 8523-PhLAM-Physique des Lasers Atomes et Molécules, F-59000 Lille, France
[3]Faculté des Sciences, Université Libre de Bruxelles (U.L.B), CP 231, Campus Plaine, B-1050 Bruxelles, Belgium

[a)]**Author to whom correspondence should be addressed:** michel.ferre.diaz@gmail.com

ABSTRACT

Two-dimensional arrays of coupled waveguides or coupled microcavities allow us to confine and manipulate light. Based on a paradigmatic envelope equation, we show that these devices, subject to a coherent optical injection, support coexistence between a coherent and incoherent emission. In this regime, we show that two-dimensional chimera states can be generated. Depending on initial conditions, the system exhibits a family of two-dimensional chimera states and interaction between them. We characterize these two-dimensional structures by computing their Lyapunov spectrum and Yorke–Kaplan dimension. Finally, we show that two-dimensional chimera states are of spatiotemporal chaotic nature.

One-dimensional nonlinear coupled microcavities exhibit a rich spatiotemporal dynamics. In particular, these coupled microcavities have fully synchronized or incoherent light emission of a spatiotemporal chaotic nature. Also, depending on the initial conditions, these devices show coexistence between desynchronized and synchronized domains, often called *optical chimera states*. In this contribution, we show evidence of optical chimeras in a two-dimensional array of coupled waveguide resonators. Due to the additional degrees of freedom, the smaller localized solutions exhibit a chaotic spatiotemporal evolution—which is not the case of the one-dimensional counterpart. The Lyapunov spectrum and Yorke–Kaplan dimensions are calculated to characterize these intriguing localized states.

I. INTRODUCTION

A two-dimensional array of coupled waveguides or coupled microcavities consists of nonlinear discrete structures.[1] This configuration appears not only in photonics but also in a large variety of systems such as biological systems,[2] condensed matter physics,[3] and Bose–Einstein condensates.[4] Nonequilibrium discrete systems are drawing considerable attention both from fundamental as well as applied points of view. In particular, spatial localization of light in discrete photonic lattices has been reported,[5–7] including complex confinement of light such as random-phase solitons.[8,9] In free propagation, the spatial confinement is attributed to the balance between the discrete diffraction and the nonlinearity. However, when dealing with coupled microresonators, the dissipation of energy due to mirrors should be compensated by optical injection. This second balance renders discrete dissipative solitons more robust.[10–12]

In general, when a system exhibits a simultaneous coexistence between coherence and incoherence behavior in coupled oscillators, the resulting phenomenon is called *chimera states*.[13] Initially, this phenomenon was reported in the context of nonlocally coupled phase oscillators[13,14] and extended later on to locally coupling oscillators.[15,16] In optical systems, experimental observations of chimera states have been reported using an optoelectronic delayed feedback setup,[17] laser diodes coupled with a nonlinear saturable absorber,[18] and laser diodes subjected to a coherent polarization.[19] Recently, one-dimensional optical chimera states have been predicted in an array of coupled Kerr resonators.[20] However, to the best of our knowledge, chimera states in two spatial dimensional optical systems have received limited attention.[21] Otherwise, in two-dimensional networks of coupled neuron systems, the emergence of

chimera states has been studied,[22,23] where these states emerge from a subcritical and supercritical bifurcations, respectively.

This paper aims to investigate the formation of two-dimensional optical chimera states in an array of coupled waveguide resonators. This phenomenon occurs in a regime where a coupled waveguide resonators exhibit coexistence between a coherent and incoherent emission. These discrete structures consist of a localized complex domain embedded in a stable homogenous background. To account for 2D optical chimera states, we use a discrete version of the two-dimensional Lugiato–Lefever equation.[24] Based on this model, we show that, depending on the initial condition; this system can support a family of two-dimensional optical chimera states. Lyapunov exponents and Yorke–Kaplan dimension allow characterizing these structures. Chimera states correspond to localized spatiotemporal chaos. In the Lugiato–Lefever equation, the optical chimera states are excluded. Indeed, this dynamical behavior is a peculiarity of discrete systems.

II. ARRAY OF DRIVEN COUPLED WAVEGUIDE RESONATORS: 2D DISCRETE LUGIATO–LEFEVER MODEL

Let us consider a two-dimensional square array of coupled waveguide resonators subject to a coherent monochromatic beam. Figure 1 shows a schematic representation of the driven square lattice. Each resonator is composed of a waveguide filled by a Kerr media, with dielectric mirrors at the end-faces. Indeed, this system corresponds to a lattice of waveguide microcavities. This device can be described by the discrete Lugiato–Lefever model.[11,12] Note that this prototype model of driven coupled oscillators has been studied more in the one-dimensional configuration. Assuming that the coupling between waveguide-resonators is small in comparison with the cavity size, the intracavity field satisfies

$$\partial_T \Psi_{n,m} = E_0 - (1 + i\Delta)\Psi_{n,m} - i|\Psi_{n,m}|^2\Psi_{n,m} - i\kappa\left(\Psi_{n+1,m} + \Psi_{n-1,m} + \Psi_{n,m+1} + \Psi_{n,m-1}\right), \quad (1)$$

where $\Psi_{n,m}(T)$ is a slowly varying envelope of the electric field circulating in (n, m)-coupled resonators. Indices n (x-axis) and m (y-axis) denote the transverse coordinates of the cavities. The detuning parameter $\Delta \equiv \omega - \omega_0$ is proportional to the difference between the resonance frequency ω_0 of the cavity and the driving field frequency ω. κ characterizes the coupling strength between the cavities. Time $t = T\tau_{ph}$ is measured in the photon lifetime unit τ_{ph}. The driving field intensity is denoted by E_0. The continuous counterpart of model Eq. (1) was used to describe Kerr optical frequency combs (see Ref. 25 and references therein).

In the continuous limit, for $\Delta > \sqrt{3}$ ($\Delta < \sqrt{3}$), the transmitted intensity as a function of the input intensity E_0^2 is bistable (monostable). The homogeneous steady state undergoes a modulational instability at $E_0^2 = E_{0c}^2 \equiv 1 + (1 - \Delta)^2$ and $|\Psi_c|^2 = 1$. At this bifurcation point, the critical wavelength is $\Lambda_c^2 = [2\pi|\kappa|/(2 - \Delta)]^{1/2}$. It has been shown that, for large injected intensity, the system exhibits a spatiotemporal chaos.[27] These dynamic behaviors are persistent when one considers the respective discrete system.[20] In this type of systems, the discreteness (Peierls–Nabarro potential) allows the confinement of light. Hence,

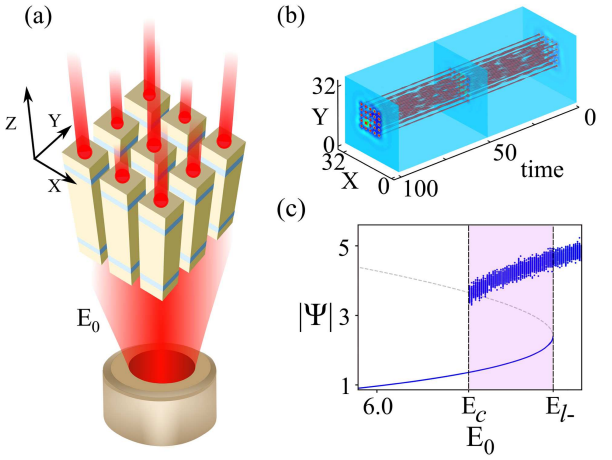

FIG. 1. Optical chimera states in a two-dimensional array of coupled microresonator. Parameters are $E_0 = 4.22$, $\Delta = 7.0$, and $\kappa = 1.876$. (a) Schematic representation of a two-dimensional array of coupled waveguide-resonators driven by an external electrical field of intensity E_0. (b) Spatiotemporal evolution of the maximum iso-surface amplitude of each interacting cavity. (c) Bifurcation diagram of model Eq. (1). The total intracavity amplitude $|\Psi|$ as a function of the pump amplitude E_0. The solid and dashed lines describe the total intracavity intensity of homogeneous steady states. The blue cloud of points shows the extreme values of the total intracavity intensity of the spatiotemporal chaotic state. The colored region accounts for the coexistence range ($E_c = 6.68 < E < E_{l-} = 7.29$). The painted area accounts for the bistability region between the homogeneous and spatiotemporal chaotic states.

the prerequisite condition for the formation of two-dimensional chimera states is the coexistence of a coherent (homogeneous state) and an incoherent state (spatiotemporal chaos) in a discrete system. Figure 1(b) displays a typical 2D chimera state in the bistability region, $E_c < E_0 < E_{l-}$. Chimera states are classified by the notation $n \times m$, which depicts the number of cavities that shows the maximum amplitude. Numerical simulations are conducted using a finite difference code with a 4th-order Runge–Kutta scheme and Neumann boundary conditions. Contrary to the continuous limit, the 2D chimera states neither grow in spite of available free space in the transverse plane nor shrink in spite of weak coupling between resonators. Figure 1(c) shows the bifurcation diagram of model Eq. (1). We plot the maximum values of the normalized total intracavity amplitude $|\Psi|$ as a function of injected field amplitude E_0. The normalized total amplitude of the intracavity field is defined as, $|\Psi(t)| = \sqrt{\sum_{i,j=1}^{N} |\Psi_{i,j}(t)|^2}/N^2$, with N^2 being the total number of coupled cavities in the lattice.

For small E_0, only a homogeneous steady state exists as a stable solution. In this case, all cavities have the same intracavity field amplitude. Increasing the input parameter up to $E_0 \geqslant E_{l-}$, the homogeneous steady state suffers a saddle-node instability. The system develops the emergence of spatiotemporal chaos.[27] Further increasing E_0, the complex dynamics keeps up. When decreasing E_0, the spatiotemporal complex dynamics perseveres until E_0 reaches E_c [see Fig. 1(c)]. For $E_0 < E_c$, the homogeneous steady state is the only

extended stationary equilibrium. Indeed, the system presents a subcritical bifurcation at $E_0 = E_c$. The coexistence is prerequisite for the formation scenario of chimera states we have previously proposed in 1D.[15]

The first finding is that the family of chimera states generated in the transverse section of the intracavity field is much more diverse than the one-dimensional case, thanks to the large variety of 2D geometrical plots. However, for the sake of simplicity, we limit our analysis to chimera states with incoherent domains forming a square as depicted in Fig. 3(a). These chimera states are characterized by spatial confinement of large temporal fluctuations (see video in the supplementary material).

III. CHARACTERIZATION OF 2D OPTICAL CHIMERA STATES

The one-dimensional version of Eq. (1) exhibits stationary localized discrete objects, *discrete cavity solitons*.[10–12] These solutions are persistent in two dimensions.[21] Depending on initial conditions, a family of discrete solutions of different sizes are observed. Increasing the driving field E_0, these localized structures present transitions from stationary, oscillatory to complex spatiotemporal states. To shed light on the mechanism of these bifurcations, we calculate the total intracavity intensity of the localized states, defined as

$$||\Psi||(t) \equiv \sum_{n,m=0}^{N} |\Psi_{n,m}(t)|^2. \tag{2}$$

Let us introduce the following terminology for localized states $n \times m$, where $n \times m$ accounts for the number of cavities that shows the maximum amplitude. For the sake of simplicity, we only considered two $n \times m$ localized states, 2×2 and 5×5. The insets in Fig. 2 show a typical snapshot of these states. Likewise, the bifurcation diagram of these localized states is shown in Fig. 2. In the top panel, the maximum total intracavity intensity $||\Psi||_{max}$ vs the driving field E_0 is presented. The blue and red dots account for the maximum total intracavity intensity for 2×2 and 5×5 states numerically obtained from Eq. (2), respectively.

Increasing the driving field, in both cases, we recognize three different regions. The first one corresponds to the stationary states, where $||\Psi||_{max}$ shows only one value. The second region is characterized by $||\Psi||_{max}$ alternates between two values for a given E_0. Indeed, this accounts for the emergence of oscillatory behavior of the localized structures. This transition corresponds to an Andronov–Hopf bifurcation. Finally, in the third region, $||\Psi||_{max}$ acquires different values in a complex manner. Namely, this is represented as a points cloud (see Fig. 2). Hence, $||\Psi||$ displays a complex temporal evolution. A further characterization of $||\Psi||$ is performed by the calculation of the power spectrum $S[\omega]$. The bottom panels shows $S[\omega]$. From these spectra, we infer a transition from stationary, oscillatory to chaotic behavior. This transition is recognized as the *period-doubling* route to chaos.[26] Indeed, this is the mechanism behind the emergence of discrete localized complex spatiotemporal chaotic structures, *optical chimera states*.

In dynamical systems theory, Lyapunov exponents constitute the most adequate tool to characterize the nature of complex spatiotemporal dynamics described above. These exponents provide

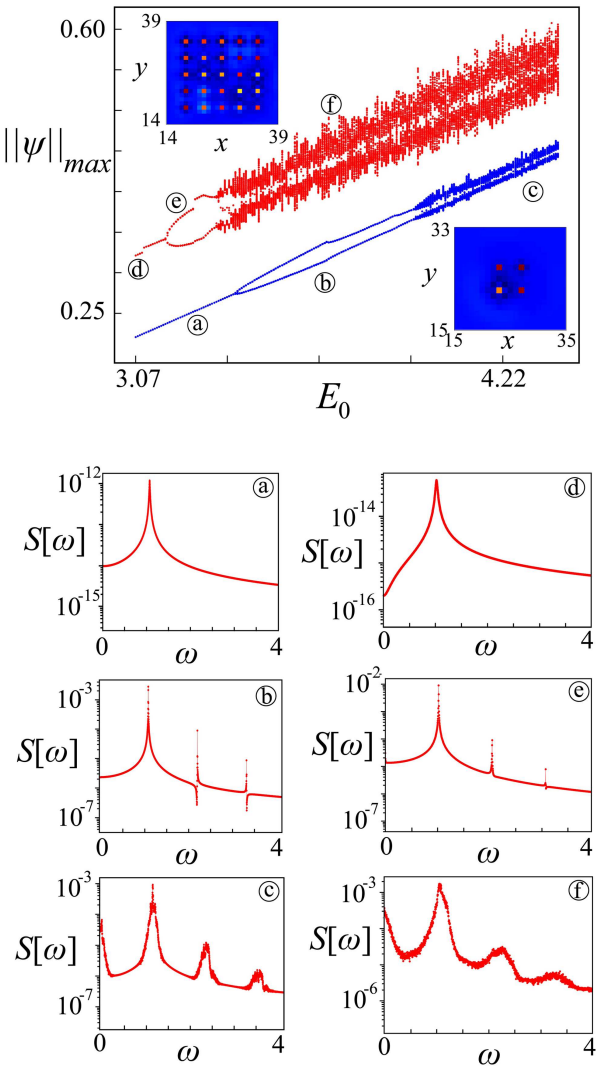

FIG. 2. Bifurcation diagram of 2×2 and 5×5 optical chimera states. The top panel shows the maximum total intracavity intensity $||\Psi||_{max}$ vs the driving field intensity E_0. The blue and red curve correspond to 2×2 and 5×5 optical chimera state, respectively. The left and right bottom panels show, respectively, the power spectrum of 2×2 and 5×5 of optical chimera state obtained in the driven field intensity indicated in the top panel.

information about sensitivity to the initial conditions, fluctuations, and complexity of solutions.[28] Low-dimensional and spatiotemporal chaos are characterized by positive Lyapunov exponents. These exponents can be computed from the method proposed by Skokos.[29] The set of Lyapunov exponents constitutes the Lyapunov spectrum $\{\lambda_i\}$ with $i = \{1, 2, \ldots, N^2\}$, $\lambda_i \leqslant \lambda_j$ and $i \leqslant j$. Low-dimensional chaos possesses a discrete Lyapunov spectrum, while spatiotemporal chaos has a continuous one. Figure 3(b) shows Lyapunov spectra of

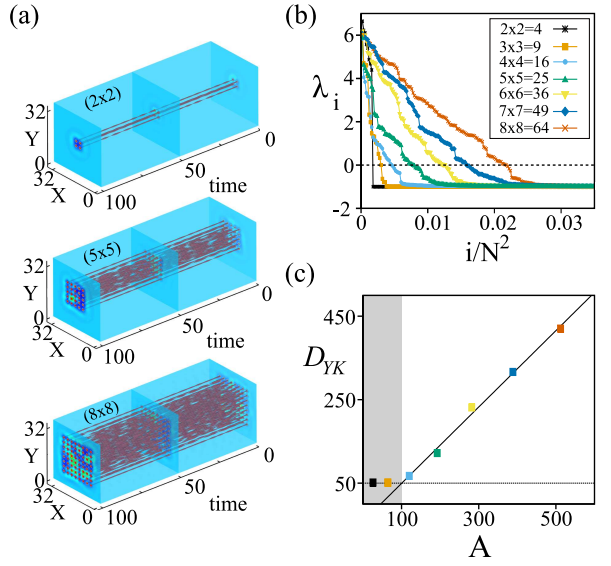

FIG. 3. Family of two-dimensional optical chimera states of model Eq. (1) with the same parameters as (a) Spatiotemporal diagrams of 2×2, 5×5, and 8×8 optical chimera states. The product $n \times m$ accounts for the number of cavities that shows the maximum amplitude. (b) Lyapunov spectra of different 2D optical chimera states obtained from Eq. (1). $\{\lambda_i\}$ denotes the i-Lyapunov exponent, $i = \{1, \ldots, N\}$ and N accounts for the total number of cavities. Each curve corresponds to the Lyapunov spectrum of the respective $n \times m$ chimera states. (c) Yorke–Kaplan dimension of the spatiotemporal chaotic solution as a function of A parameter. This parameter accounts for the average number of microcavities in the incoherence domain.

different optical chimera states. From this plots, we see that positive Lyapunov exponents increase with the size of chimera states. Hence, the complexity of these localized solutions increase with the size of chimera states.

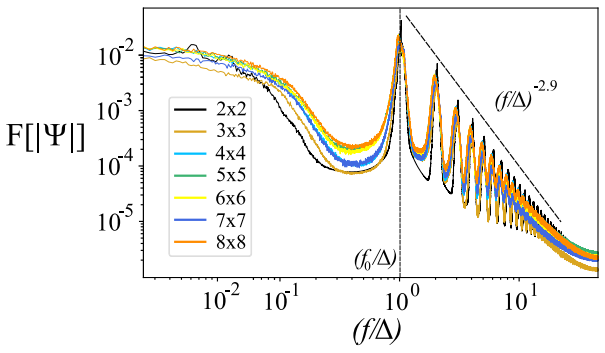

FIG. 4. Power spectrum $F[|\Psi|]$ of a single waveguide-resonator cavity as a function of frequency f and the detuning parameter Δ. At high frequencies, the power spectrum shows a power law $f^{-2.9}$ which is a signature of turbulence-like dynamics.

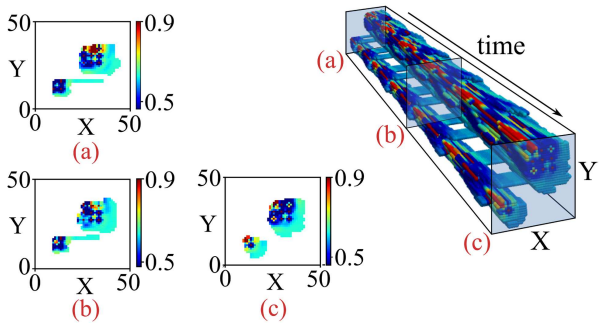

FIG. 5. 2D chimera states exist together. Spatiotemporal diagram of 2D chimera states in an array of coupled waveguide-resonator cavities. The color bar stands for the intracavity intensity field. Insets in (a)–(c) account for the cross section at different times.

In addition, from Lyapunov spectrum we can compute the Yorke–Kaplan dimension defined by $D_{YK} = p + \sum_{i=1}^{p} \lambda_i / |\lambda_{p+1}|$, where p is the largest integer for which $\lambda_1 + \cdots + \lambda_p > 0$. Figure 3(c) shows the Yorke–Kaplan dimension of different chimera solutions. From small values of A, the Yorke–Kaplan dimension remains constant, where A denotes the average number of microcavities in the incoherence domains. As A is increased, the Yorke–Kaplan dimension grows. This feature is the manifestation of the extensive property of this dynamical dimension,[28] indicating that 2D optical chimera states belong to the class of spatiotemporal chaos.

Fourier analysis is used to further characterize the underlying dynamics of chimera states. To perform this analysis, we have the spectral density of the signal recorded at the location of one of the largest local maxima in the incoherent domain. Figure 4 shows the resulting power spectrum for different chimera states. The shape of the power spectrum is not affected by the size of the incoherence domain. The power spectrum has a dominant peak at the value of the detuning parameter. For high frequencies, the power spectrum presents a power f^n where $n = -2.932$, which is a signature of turbulence-like behavior.[30]

Finally, numerical simulations of model Eq. (1) show evidence of the coexistence between dissimilar chimera states simultaneously in different spatial locations in the transverse plane. An example of such a behavior is shown in Fig. 5, where 2×2 and 3×3 optical chimera states exist together. Insets account for the cross section at different times. The 2D spatiotemporal diagram suggests that the chimera states interact weakly.

IV. CONCLUSION

We have shown evidence of two-dimensional optical chimera states in a driven array of locally coupled passive Kerr optical resonators. Adequate initial conditions have been used to generate a family of these solutions. The main characteristic of these solutions is spatial confinement of light in the transverse plane involving complex multi-peak dynamics. Besides, we have shown that these solutions can coexist together. The 2D chimera states are inherent

to the discrete nature of the system. Indeed, in the continuous limit, these states are unstable. We have characterized these solutions by computing Lyapunov spectra, Yorke–Kaplan dimensions, and the power spectrum. We have showed that the 2D optical chimera states belong to the class of spatiotemporal chaos and turbulence-like behaviors. The prerequisite condition for their formation requires a bistable behavior between homogeneous background and spatiotemporal chaos. This condition is rather general, and, therefore, this prediction is important for the identification and understanding of the various complex spatiotemporal behaviors observed in practical systems.

SUPPLEMENTARY MATERIAL

See the supplementary material for supporting contents.

ACKNOWLEDGMENTS

M.G.C. and M.A.F. acknowledge financial support of Millennium Institute for Research in Opticsan Fondecyt (No. 1180903). M.T. is a Research Director of the Fonds National de la Recherche Scientifique (Belgium). S.C. acknowledges the LABEX CEMPI (No. ANR-11-LABX-0007) as well as the Ministry of Higher Education and Research, Hauts de France council, and European Regional Development Fund (ERDF) through the Contract de Projets Etat-Region (CPER Photonics for Society P4S).

REFERENCES

[1] D. N. Christodoulides and R. I. Joseph, Opt. Lett. **13**, 794 (1988).
[2] A. S. Davydov and N. I. Kislukha, Phys. Status Solidi B **59**, 465–470 (1973).
[3] W. P. Su, J. R. Schieffer, and A. J. Heeger, Phys. Rev. Lett. **42**, 1968–1971 (1979).
[4] A. Trombettoni and A. Smerzi, Phys. Rev. Lett. **84**, 5435–5438 (2001).
[5] D. N. Christodoulides, F. Lederer, and Y. Silberberg, Nature **424**, 817 (2003); R. Morandotti, U. Peschel, J. S. Aitchison, H. S. Eisenberg, and Y. Silberberg, Phys. Rev. Lett. **81**, 3383 (1999).
[6] J. W. Fleischer, M. Segev, N. K. Efremidis, and D. N. Christodoulides, Nature **422**(6928) 147 (2003); N. K. Efremidis, S. Sears, D. N. Christodoulides, J. W. Fleischer, and M. Segev, Phys. Rev. E **66**, 046602 (2002); D. Neshev, E. Ostrovaskaya, Y. Kivshar, and W. Krolikowski, Opt. Lett. **28**, 710 (2003).
[7] A. Fratalocchi, G. Assanto, K. A. Brzdakiewicz, and M. A. Karpierz, Opt. Lett. **29**, 1530 (2004); Y. V. Kartashov, V. A. Vysloukh, Opt. Lett. **30**, 637 (2005); H. Martin, E. D. Eugenieva, Z. Chen, and D. N. Christodoulides, Phys. Rev. Lett. **92**, 123902 (2004); B. A. Malomed and P. G. Kevrekidis, Phys. Rev. E **64**, 026601 (2001).
[8] O. Cohen, G. Bartal, H. Buljan, T. Carmon, J. W. Fleischer, M. Segev, and D. N. Christodoulides, Nature **433**, 500 (2005).
[9] H. Buljan, O. Cohen, J. W. Fleischer, T. Schwartz, M. Segev, Z. H. Musslimani, N. K. Efremidis, and D. N. Christodoulides, Phys. Rev. Lett. **92**, 223901 (2004).
[10] U. Peschel, O. Egorov, and F. Lederer, Opt. Lett. **29**, 1909 (2004).
[11] O. Egorov, U. Peschel, and F. Lederer, Phys. Rev. E **71**, 056612 (2005).
[12] O. A. Egorov and F. Lederer, Opt. Lett. **38**, 1010 (2013).
[13] D. M. Abrams and S. H. Strogatz, Phys. Rev. Lett. **93**, 174102 (2004).
[14] Y. Kuramoto and D. Battogtokh, Nonlinear Phenom. Complex Syst. **5**, 380 (2002).
[15] M. G. Clerc, S. Coulibaly, M. Ferré, M. A. García-Ñustes, and R. G. Rojas, Phys. Rev. E **93**, 052204 (2016).
[16] M. G. Clerc, S. Coulibaly, M. A. Ferré, and R. G. Rojas, Chaos **28**, 083126 (2018).
[17] L. Larger, B. Penkovsky, and Y. Maistrenko, Nat. Commun. **6**, 7752 (2015).
[18] E. A. Viktorov, T. Habruseva, S. P. Hegarty, G. Huyet, and B. Kelleher, Phys. Rev. Lett. **112**, 224101 (2014).
[19] C.-H. Uy, L. Weicker, D. Rontani, and M. Sciamanna, APL Photon. **4**, 056104 (2019).
[20] M. G. Clerc, M. A. Ferré, S. Coulibaly, R. G. Rojas, and M. Tlidi, Opt. Lett. **42**, 2906 (2017).
[21] K. M. Aghdami, M. Golshani, and R. Kheradmand, IEEE Photon. J. **4**, 1147 (2012).
[22] A. Schmidt, T. Kasimatis, J. Hizanidis, A. Provata, and P. Hövel, Phys. Rev. E **95**, 032224 (2017).
[23] S. Kundu, S. Majhi, B. K. Bera, D. Ghosh, and M. Lakshmanan, Phys. Rev. E **97**, 022201 (2018).
[24] L. A. Lugiato and R. Lefever, Phys. Rev. Lett. **58**, 2209 (1987).
[25] Y. K. Chembo, D. Gomila, M. Tlidi, and C. R. Menyuk, Eur. Phys. J. D **71**, 299 (2017).
[26] P. Bergé, Y. Pomeau, and C. Vidal, *Order within Chaos* (Hermann, 1987).
[27] Z. Liu, M. Ouali, S. Coulibaly, M. G. Clerc, M. Taki, and M. Tlidi, Opt. Lett. **42**, 1063 (2017).
[28] A. Pikovsky and A. Politi, *Lyapunov Exponents: A Tool to Explore Complex Dynamics* (Cambridge University, 2016).
[29] C. H. Skokos, "The Lyapunov characteristic exponents and their computation," in *Dynamics of Small Solar System Bodies and Exoplanets* (Springer, 2010), pp. 63–135.
[30] U. Frisch and A. N. Kolmogorov, *Turbulence: The Legacy of AN Kolmogorov* (Cambridge University Press, 1995).